Desalination and Water Treatment
www.deswater.com
doi: 10.5004/dwt.2022.28166

250 (2022) 189–196
February

High hydrogen production rate from potassium borohydride hydrolysis with an efficient catalyst: CNT@Ru(0)

M. Salih KESKIN[a,*], Mehmet Salih AĞIRTAŞ[b], Orhan BAYTAR[c], M. Sait İZGI[c], Ömer ŞAHIN[c], Sabit HOROZ[d]

[a]*Department of Basic Education, Faculty of Education, Siirt University, Siirt, Turkey, email: msalih.keskin@gmail.com*
[b]*Department of Chemistry, Faculty of Science, Van Yuzuncu Yıl University, 65080 Van, Turkey, email: agirtas65@yyu.edu.tr*
[c]*Department of Chemistry, Faculty of Arts and Sciences, İstanbul Technical University, Turkey, emails: orhanbaytar@siirt.edu.tr (O. BAYTAR), saitizgi@siirt.edu.tr (M. Sait İZGI), omersahin@itu.edu.tr (Ö. ŞAHIN)*
[d]*Department of Metallurgy and Materials Engineering, Faculty of Engineering and Natural Sciences, Sivas University of Science and Technology, Siirt 56100, Turkey, email: sabit.horoz@sivas.edu.tr*

Received 13 September 2021; Accepted 12 January 2022

ABSTRACT

We describe the production and catalytic activity of a carbon nanotube supported-Ru(0) (CNT@Ru(0)) catalyst. For the first time, the produced CNT@Ru(0) catalyst is used to achieve the greatest hydrogen production rate from potassium borohydride (KBH_4) hydrolysis. The produced CNT@Ru(0) catalyst shows promise in the creation of hydrogen from the degradation of KBH_4. The hydrogen generation rate of CNT@Ru(0) is determined to be 86,264.85 mL min^{-1} can with a low activation energy of 30.18 kJ mol^{-1}. CNTs are potential support for distributing metal catalysts, according to the current work. Furthermore, structural, morphological, and elemental characteristics of the produced CNT@Ru(0) catalyst are investigated.

Keywords: Catalyst; Ruthenium; Hydrogen; Potassium borohydride

1. Introduction

In the use of hydrogen energy, secure storage and the effective release of hydrogen are critical [1,2]. Materials that can retain enough hydrogen in terms of gravimetric and volumetric densities, as well as have acceptable thermodynamic and kinetic characteristics, have been the subject of intense study and development [3]. Long-term research has demonstrated that solid media, such as sorbent materials or hydrides, are the most effective and safest means of storing hydrogen [4,5].

$NaBH_4$ is a chemical hydride that is stable and easy to handle when compared to other chemical hydrides [6–9]. At room temperature, the hydrolysis reaction of $NaBH_4$ and H_2O liberates just a small proportion of the theoretical quantity of hydrogen, although the hydrolysis is expedited by the application of catalysts [10]. Both sodium borohydride ($NaBH_4$) and potassium borohydride (KBH_4) are safe and effective hydrogen storage compounds, but in the solid form, both are susceptible to moisture in the air [11,12]. KBH_4 can be used to reduce aldehydes, ketones, acid chlorides, and anhydrides in the same way as $NaBH_4$ can. Because of its strong reactivity, hydrogen concentration, and potential, it is also utilized in vitamin A production and as a fuel for fuel cells [13]. The reaction of $NaBH_4$ with KOH is commonly used to make KBH_4 [14,15]. KBH_4 may also be made utilizing saline hydrides and dehydrated borates in a mechano-chemical process at ambient temperature.

Thermal dehydrogenation or solvolysis can both liberate hydrogen from the KBH_4 compound. Because the

* Corresponding author.

dehydrogenation temperature is so high, catalytic methanolysis and hydrolysis of KBH_4 utilizing transition metal catalysts such as platinum, ruthenium, rhodium, palladium, iron, cobalt, and nickel have sparked a lot of interest [16–22]. Despite employing the greatest stabilizers, most of these transition metal catalysts are in the form of nanoparticles, which suffer from long-term stability due to aggregating into clumps and eventually to the bulk metal, resulting in a reduction in catalytic activity and lifespan [23]. In systems with restricted void spaces, such as zeolite, the use of nanocluster catalysts has been proven to be an effective means of avoiding aggregation. The zeolite confined metal(0) nanoclusters catalysts have two significant drawbacks [24–26]: diffusion-controlled kinetics and metal migration to the external surface at high temperatures, notwithstanding their high activity and extended lifespan [27–32]. When compared to traditional catalyst supports, carbon nanotubes appear to be very appealing as catalyst supports in liquid phase reactions because they provide high dispersion of nanoparticles, significantly increase the contact surface between the reactants and active sites, and greatly reduce diffusion limitations [33]. Various examples of carbon-nanotube-supported ruthenium catalysts have been reported, including those formed by impregnation of ruthenium on carbon nanotubes with a high Ru/C ratio of 1:1 at high temperature, or those formed by using additional reducing agents such as hydrogen at high temperature or ethylene glycol [34]. The catalyst materials may be altered as a result of the high-temperature treatment, and the high ruthenium loading leads to the production of large nanoparticles.

In this study, carbon nanotube supported-Ru(0) (CNT@Ru(0)) catalyst, which was not used in KBH_4 hydrolysis before, was synthesized by the chemical precipitation and reduction method. The effects of parameters such as Ru/CNT ratio, KOH concentration, catalyst amounts, KBH_4 concentration, and temperature on the hydrolysis of KBH_4 were examined and the obtained observations were interpreted. The degree of reaction and the activation energy was also calculated.

2. Experimental study

2.1. Materials

Ruthenium(III) chloride trihydrate ($RuCl_3{\cdot}3H_2O$) and sodium borohydride ($NaBH_4$, 97.0 wt.%) from Shanghai Aibi Chemistry Preparation Co. Ltd., China, were used without further purification.

2.2. Catalyst preparation

The catalysts were prepared by the impregnation-chemical reduction method. In a typical preparation procedure, CNT@Ru(0) catalysts were prepared by impregnation of the carbon nanotube (CNT) (a diameter of 150 nm was purchased from Electrovac) with an aqueous mixture solution containing $RuCl_3{\cdot}3H_2O$ (0.5 g). To reduce the metal salts to alloy nanoparticles, a predetermined quantity of 5 wt.% $NaBH_4$ was dropped into the catalyst precursor after drying. The sample was then filtered, washed multiple times with distilled water, and dried for 10 h at 373 K. Finally, the catalyst was calcined for 2 h at 673 K in a nitrogen environment.

2.3. Characterization

X-ray diffraction (XRD, Rigaku X-ray diffractometer), scanning electron microscopy (SEM, JEOL JSM 5800), and energy-dispersive X-ray spectroscopy (EDS, JEOL JSM 5800) measurements were performed to investigate the characteristics of the produced CNT@Ru(0) catalyst.

2.4. Catalyst testing

The catalyst testing was carried out using KBH_4. The kinetic experiments with catalysts were carried out in batches, with the reactor being a 50 mL three-necked round-bottom flask. A thermometer was placed into the fluid via the left-neck port to monitor the temperature. In a typical hydrogen production experiment, 10 mL of 2 wt.% KBH_4 + 0 wt.% KOH was placed in the flask first.

3. Results and discussion

3.1. Results of characterization

The XRD patterns of the CNT@Ru(0) catalyst are given in Fig. 1. The peaks that appeared at 26.2°, 43.3°, and 54.5° may be classified as (002), (100), and (004) carbon structure reflections, respectively [35]. In Fig. 1, there is no visible peak attributed to Ru-metal, owing to the low Ru loading of CNT@Ru(0) catalyst.

Fig. 2a and b show the SEM image and SEM-EDS spectrum of the CNT@Ru(0) catalyst, indicating that the low ruthenium loading posed no threat to the carbon nanotube wall, which is consistent with XRD data, and Ru seems to be the only component identified in the sample.

3.2. Results of catalyst testing

3.2.1. Effect of different Ru(0) concentration

The graphs of hydrogen volume vs. time and hydrogen production rate vs. Ru(0) concentration in the presence of different Ru(0) concentrations (2.5%, 5%, 7.5%, 10%, and 20%) are exhibited in Fig. 3. Experimental conditions were

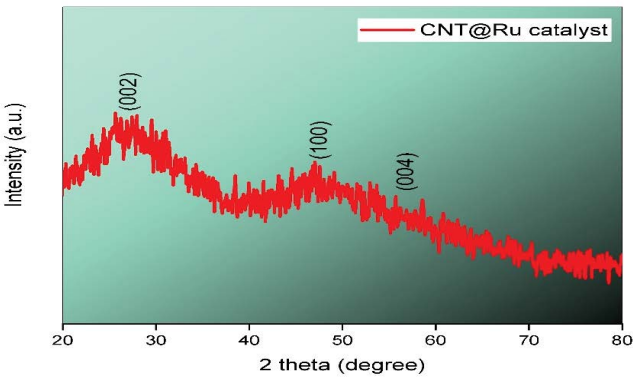

Fig. 1. XRD patterns of CNT@Ru(0) catalyst.

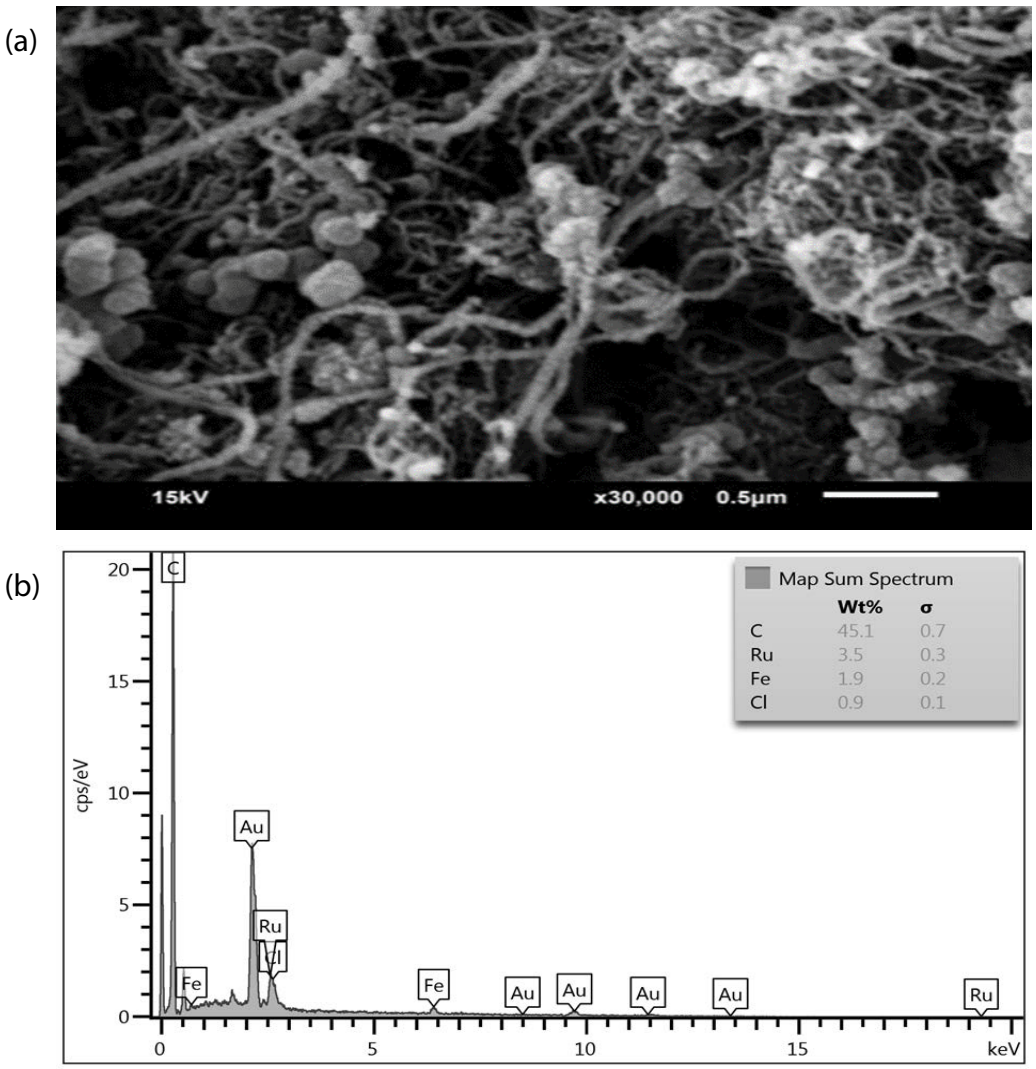

Fig. 2. (a) SEM image of CNT@Ru(0) catalyst and (b) SEM-EDS spectrum of CNT@Ru(0) catalyst.

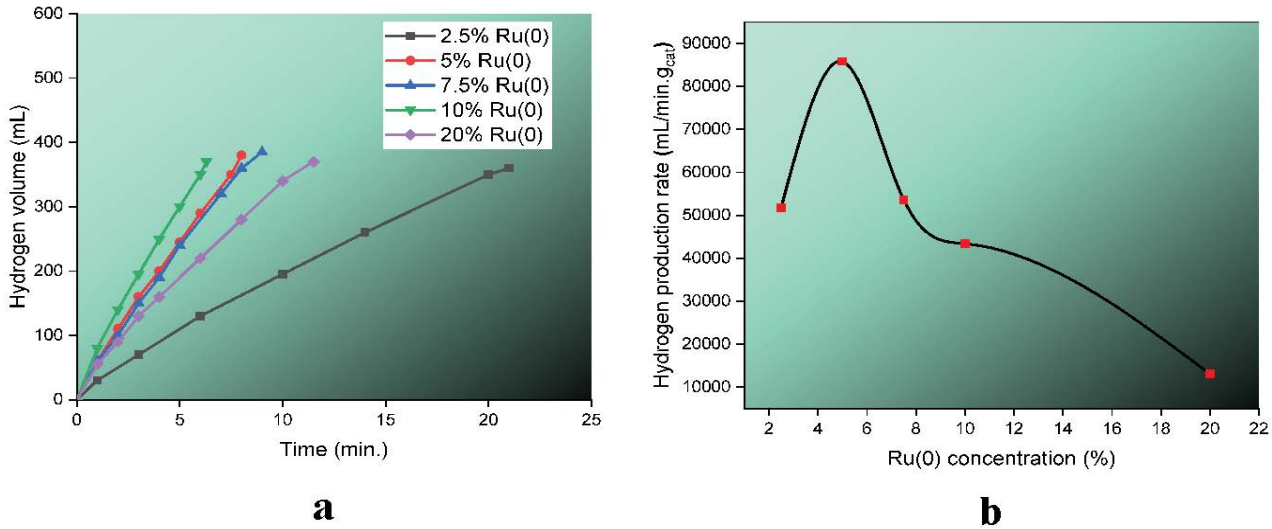

Fig. 3. Effect of Ru(0) concentration on the hydrogen production in the presence of different Ru(0) concentrations: (a) hydrogen volume vs. time and (b) hydrogen production rate vs. Ru(0) concentration (%).

set at 30°C + 2 wt.% KBH_4 + 0 wt.% KOH + 0.02 g catalyst amount.

The completion times of KBH_4 hydrolysis in the presence of 2.5%, 5%, 7.5%, 10%, and 20% of Ru(0) concentration were determined as 21.01, 8.03, 8.98, 6.29, and 11.54 min, respectively. In the presence of 2.5%, 5%, 7.5%, 10%, and 20% of Ru(0) concentration, hydrogen production rates were 51,553.26, 86,264.85, 53,743.63, 43,327.67, and 12,716.46 mL/min g_{cat}, respectively. It should be noted that the increase in Ru(0) concentration causes a decrease in the hydrogen production rate. The catalytic activity of the CNT@Ru(0) catalyst diminishes as the Ru loading rises, most likely owing to the clumping of nanostructures, leading to a reduction in surface area and availability of catalyst surface.

3.2.2. Effect of catalyst amount

The graphs of hydrogen volume vs. time and hydrogen production rate vs. catalyst amount in the presence of different amounts (0.01, 0.02, 0.04, and 0.06 g) of CNT@Ru(0) catalysts are exhibited in Fig. 4. Experimental conditions were set at 30°C + 2 wt.% KBH_4 + 0 wt.% KOH.

The completion times of KBH_4 hydrolysis in the presence of 0.01, 0.02, 0.04, and 0.06 g of CNT@Ru(0) catalyst were determined as 22.98, 8.03, 4.01, and 2.19 min, respectively. In the presence of 0.01, 0.02, 0.04, and 0.06 g of CNT@Ru(0) catalyst catalysts, hydrogen production rates were 59,875.49, 86,264.85, 83,701.18 and 141,595.92 mL/min g_{cat}, respectively. The impact of catalyst amount on catalytic activity is so strong that even a little amount of catalyst may double the activity of the CNT@Ru(0) catalyst. The rate of hydrogen production rises as the catalyst amount rises. These findings indicate that the catalyst amount may be used to influence the rate of hydrogen production.

3.2.3. Effect of KOH concentration

KOH plays an important role in the hydrolysis of chemical hydrides, such as providing stabilization. Fig. 5 reveals the graphs of hydrogen volume vs. time and hydrogen production rate vs. KOH concentration (%) in the presence of different KOH concentrations (0%, 0.1%, 0.3%, and 0.5%). Experimental conditions were set at 30°C + 2 wt.% KBH_4 + 0.02 g catalyst amount.

The completion times of KBH_4 hydrolysis in the presence of 0%, 0.1%, 0.3%, and 0.5% of KOH concentration were determined as 8.03, 11.02, 12.01, and 16.07 min, respectively. In the presence of 0%, 0.1%, 0.3%, and 0.5% of KOH concentration, hydrogen production rates were 86,264.85, 65,042.44, 48,205.99 and 46,819.46 mL/min g_{cat}, respectively. It should be noted that the increase in KOH concentration causes a decrease in the hydrogen production rate. It is thought that hydroxyl ions caused by the increase in KOH concentration form a bi-functional surface reaction during direct adsorption to the surface of the catalyst. Thus, excessive OH concentration adversely affects the hydrolysis reaction and hydrogen production rate.

3.2.4. Effect of KBH_4 concentration

The graphs of hydrogen volume vs. time and hydrogen production rate vs. KBH_4 concentration in the presence of different KBH_4 concentrations (1%, 2%, 4%, and 7%) are exhibited in Fig. 6. Experimental conditions were set at 30°C + 0.02 g catalyst amount + 0 wt.% KOH.

The completion times of KBH_4 hydrolysis in the presence of 1%, 2%, 4%, and 7% of KBH_4 concentration were determined as 6.89, 8.03, 26.86, and 75.13 min, respectively. In the presence of 1%, 2%, 4%, and 7% of KBH_4 concentration, hydrogen production rates were 44,851.44, 86,264.85, 54,313.80 and 39,808.99 mL/min g_{cat}, respectively. This is sensible because a greater KBH_4 concentration causes the reaction to use more water and create more hydrated by-products, which can considerably raise the viscosity of the solution, obstructing mass transfer and slowing the reaction rate. On the hydrolysis of $NaBH_4$, a similar phenomenon has been discovered [36]. In addition, several

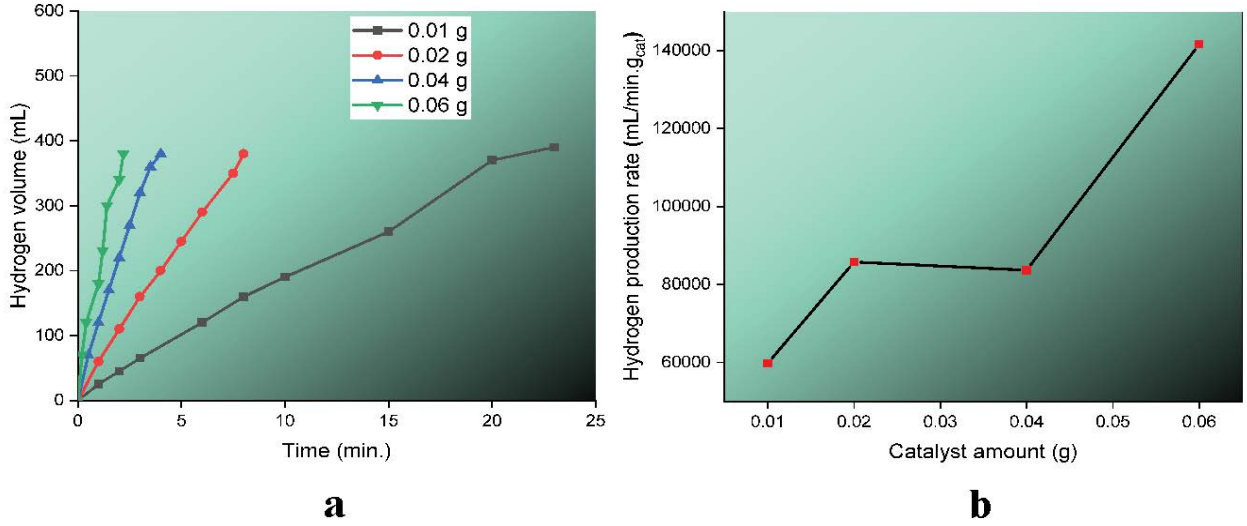

Fig. 4. Effect of catalyst amount on the hydrogen production in the presence of different CNT@Ru(0) catalyst amounts: (a) hydrogen volume vs. time and (b) hydrogen production rate vs. catalyst amount (g).

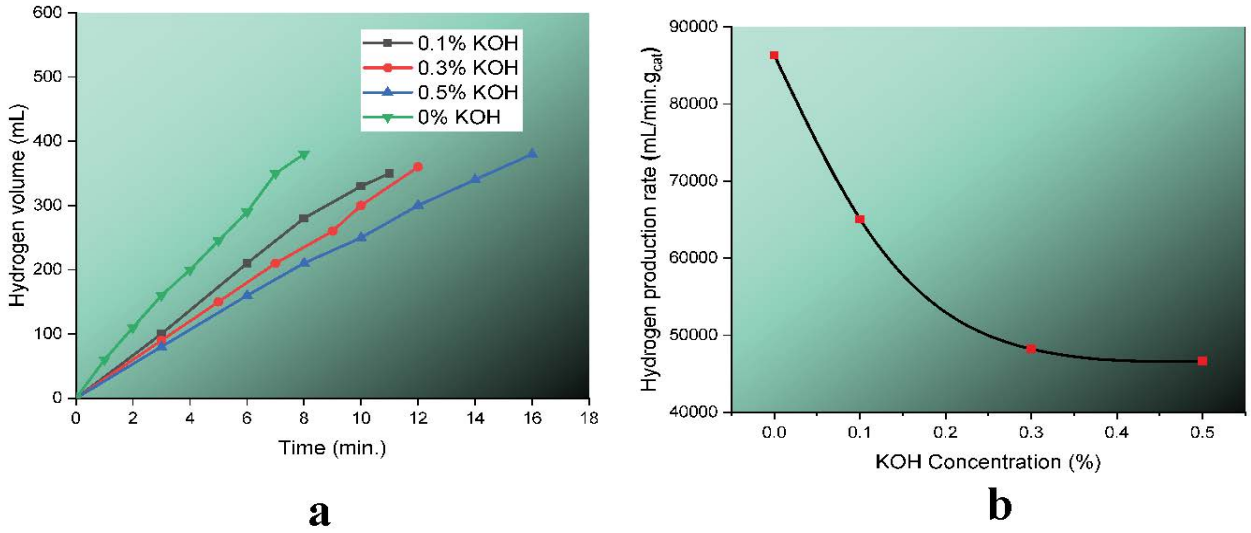

Fig. 5. Effect of KOH concentration on the hydrogen production in the presence of different KOH concentrations: (a) hydrogen volume vs. time and (b) hydrogen production rate vs. KOH concentration (%).

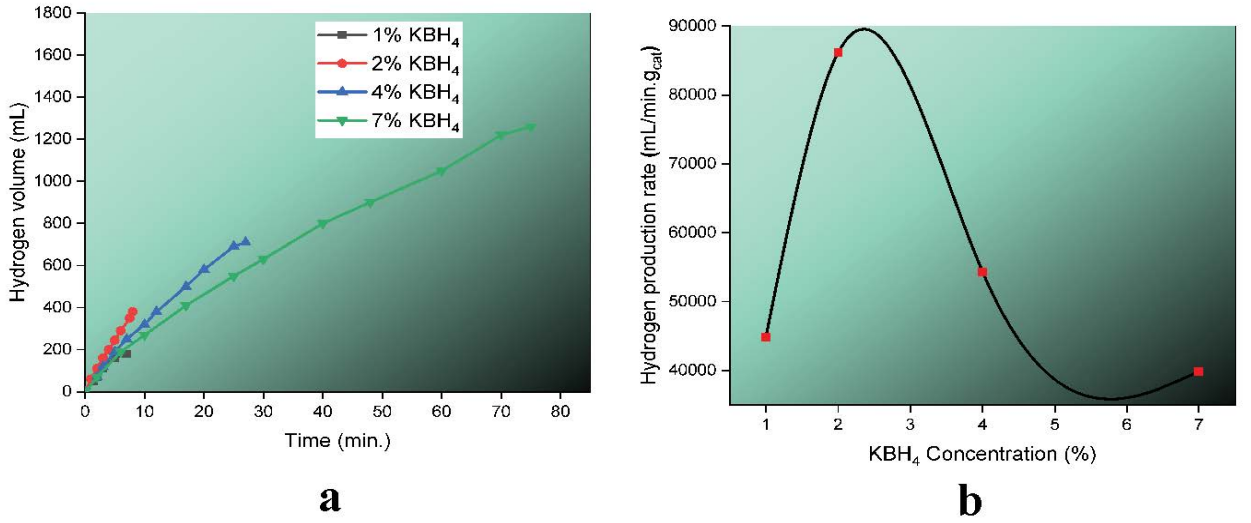

Fig. 6. Effect of KBH_4 concentration on the hydrogen production in the presence of different KBH_4 concentrations: (a) hydrogen volume vs. time and (b) hydrogen production rate vs. KBH_4 concentration (%).

types of literature have documented a reduction in hydrogen production rate as a function of $NaBH_4$ content [37,38].

3.2.5. Effect of temperature

Fig. 7 demonstrates the graphs of hydrogen volume vs. time and hydrogen production rate vs. temperature at different temperatures (20°C, 30°C, 40°C, and 50°C). Experimental conditions were set at 2 wt.% KBH_4 + 0 wt.% KOH + 0.02 g catalyst amount.

The completion times of KBH_4 hydrolysis at 20°C, 30°C, 40°C, and 50°C were determined as 23.01, 8.03, 3.97, and 2.16 min, respectively. At 30°C, 40°C, 50°C, and 60°C, hydrogen production rates were 35,865.87, 86,264.85, 136,566.21 and 332,449.06 mL/min g_{cat}, respectively. As can be seen from Fig. 7, one of the most effective methods to complete the hydrolysis reaction in a shorter time and to have a higher hydrogen production rate is to increase the solution temperature. It is well known that an increase in solution temperature will accelerate the hydrogen production process.

The activation energy (E_a) was calculated using the Arrhenius plot shown in Fig. 8, which was generated from the linear component of the curve for each temperature. The E_a of CNT@Ru(0) catalyst was derived as 30.18 kJ mol^{-1}, which is comparable to previously reported values for KBH_4 hydrolysis. Table 1 lists the E_a values of various previously investigated catalysts used for the hydrolysis of KBH_4 for comparison. It can be concluded that CNT@Ru(0) catalyst provides a notable E_a value. As CNTs are utilized as a

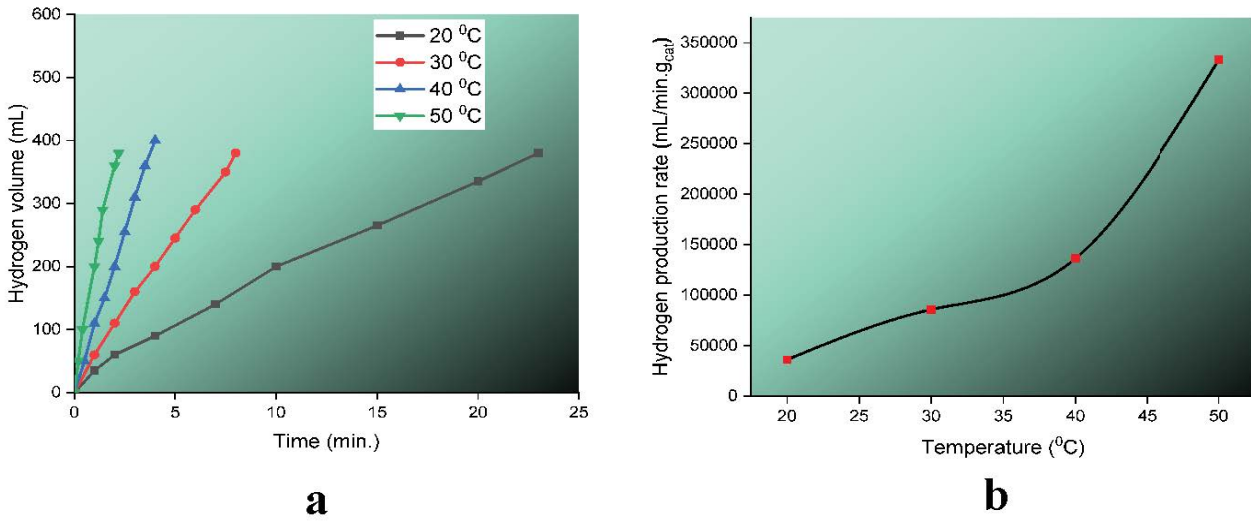

Fig. 7. Effect of temperature on the hydrogen production at different temperatures: (a) hydrogen volume vs. time and (b) hydrogen production rate vs. temperature (°C).

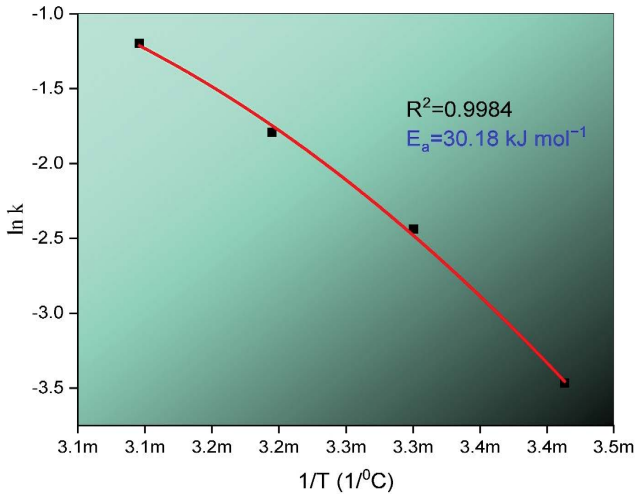

Fig. 8. The plot of ln*k* vs. 1/*T*.

support, the CNT@Ru(0) catalyst's enhanced catalytic activity can be linked to a lower mass transfer limitation in the liquid state.

4. Conclusion

As a catalyst for hydrogen generation from the hydrolysis of KBH_4, CNT@Ru(0) was produced. The CNT@Ru(0) catalyst was discovered to be capable of generating hydrogen from KBH_4. In the presence of a CNT@Ru(0) catalyst, the highest hydrogen production rate and activation energy of the hydrogen production process were 86264.85 mL/min g_{cat} and 30.18 kJ mol^{-1}, respectively. The CNT@Ru(0) catalyst was found to have a high hydrogen efficiency and a considerable reduction in the reaction time of KBH_4 hydrolysis. The mesoporous structure of CNTs is linked to the strong catalytic activity of the CNT@Ru(0) catalyst. It can be claimed that CNT@Ru(0) is an extremely impressive catalyst for on-board hydrogen generation from the hydrolysis of KBH_4 due to its high catalytic activity and easy synthesis procedure.

Table 1
The E_a values of some catalysts employed for the hydrolysis of KBH_4 at room temperature

Catalyst	E_a (kJ mol^{-1})	References
RuP_2/1.03CDs-900	43.95	[39]
$Cu_{0.2}Co_{0.8}$/HPC	41.7	[40]
Ru/carbon black	34.8	[41]
Ru/MIL-53(Al)	33.7	[42]
CNT@Ru(0)	30.18	Current study
Ru/graphene	11.7	[43]

Acknowledgments

The authors are grateful to the Research Foundation of Yüzüncü Yıl University for financial support under project FDK-2017-6256.

References

[1] K.L. Lim, H. Kazemian, Z. Yaakob, W.R.W. Daud, Solid-state materials and methods for hydrogen storage: a critical review, Chem. Eng. Technol., 33 (2010) 213–226.
[2] J. Ren, N.M. Musyoka, H.W. Langmi, M. Mathe, S. Liao, Current research trends and perspectives on materials-based hydrogen storage solutions: a critical review, Int. J. Hydrogen Energy, 42 (2017) 289–311.
[3] K.C. Kim, A review on design strategies for metal hydrides with enhanced reaction thermodynamics for hydrogen storage applications, Int. J. Energy Res., 42 (2018) 1455–1468.
[4] T. Asefa, K. Koh, C.W. Yoon, CO_2-mediated H_2 storage-release with nanostructured catalysts: recent progresses, challenges, and perspectives, Adv. Energy Mater., 9 (2019) 1901158, doi: 10.1002/aenm.201901158.

[5] F. Chang, W. Gao, J. Guo, P. Chen, Emerging materials and methods toward ammonia-based energy storage and conversion, Adv. Mater., 33 (2021) 2005721, doi: 10.1002/adma.202005721.
[6] A.A. Dafedar, S.S. Verma, A. Yadav, Hydrogen Storage Techniques for Stationary and Mobile Applications: A Review, In: Recent Advances in Sustainable Technologies, Springer, Singapore, 2021, pp. 29–40.
[7] S. Farrukh, X. Fan, K. Mustafa, A. Hussain, M. Ayoub, M. Younas, Hydrogen from Miscellaneous Sources and Nanotechnology, In: Nanotechnology and the Generation of Sustainable Hydrogen, Green Energy and Technology, Springer, Cham, 2021, pp. 61–71. Available at: https://doi.org/10.1007/978-3-030-60402-8_6
[8] S. Hosgun, M. Ozdemir, Y.B. Sahin, Optimization of hydrogen generation by catalytic hydrolysis of $NaBH_4$ with halloysite-supported CoB catalyst using response surface methodology, Clays Clay Miner., 69 (2021) 128–141.
[9] S.-m. Kwon, M.J. Kim, S. Kang, T. Kim, Development of a high-storage-density hydrogen generator using solid-state $NaBH_4$ as a hydrogen source for unmanned aerial vehicles, Appl. Energy, 251 (2019) 113331, doi: 10.1016/j.apenergy.2019.113331.
[10] Ö. Şahin, H. Dolaş, M. Özdemir, The effect of various factors on the hydrogen generation by hydrolysis reaction of potassium borohydride, Int. J. Hydrogen Energy, 32 (2007) 2330–2336.
[11] U.B. Demirci, P. Miele, Cobalt in $NaBH_4$ hydrolysis, Phys. Chem. Chem. Phys., 12 (2010) 14651–14665.
[12] J.-H. Kim, H. Lee, H.S. Cheol, H.-S. Kim, M.-S. Song, J.-Y. Lee, Production of hydrogen from sodium borohydride in alkaline solution: development of catalyst with high performance, Int. J. Hydrogen Energy, 29 (2004) 263–267.
[13] D. Xu, H. Wang, Q. Guo, S. Ji, Catalytic behavior of carbon supported Ni–B, Co–B and Co–Ni–B in hydrogen generation by hydrolysis of KBH_4, Fuel Process. Technol., 92 (2011) 1606–1610.
[14] L. Laversenne, C. Goutaudier, R. Chiriac, C. Sigala, B. Bonnetot, Hydrogen storage in borohydrides comparison of hydrolysis conditions of $LiBH_4$, $NaBH_4$ and KBH_4, J. Therm. Anal. Calorim., 94 (2008) 785–790.
[15] J.-X. Liu, M. Yang, R.-F. Jiang, X.-C. Zheng, P. Liu, Hexagonal boron nitride supported ruthenium nanoparticles as highly active catalysts for ammonia borane hydrolysis, Int. J. Hydrogen Energy, 46 (2021) 17708–17719.
[16] S. Akbayrak, S. Özkar, Cobalt ferrite supported platinum nanoparticles: superb catalytic activity and outstanding reusability in hydrogen generation from the hydrolysis of ammonia borane, J. Colloid Interface Sci., 596 (2021) 100–107.
[17] F. Akti, Hydrogen generation from hydrolysis of sodium borohydride by silica xerogel supported cobalt catalysts: positive roles of amine modification and calcination treatment, Fuel, 303 (2021) 121326.
[18] A.F. Baye, M.W. Abebe, R. Appiah-Ntiamoah, H. Kim, Engineered iron-carbon-cobalt (Fe_3O_4@C-Co) core-shell composite with synergistic catalytic properties towards hydrogen generation via $NaBH_4$ hydrolysis, J. Colloid Interface Sci., 543 (2019) 273–284.
[19] H.C. Brown, C.A. Brown, New, highly active metal catalysts for the hydrolysis of borohydride, J. Am. Chem. Soc., 84 (1962) 1493–1494.
[20] D. Kilinc, O. Sahin, Ruthenium-Imine catalyzed KBH_4 hydrolysis as an efficient hydrogen production system, Int. J. Hydrogen Energy, 46 (2021) 20984–20994.
[21] Q. Yao, Z.-H. Lu, Y. Yang, Y. Chen, X. Chen, H.-L. Jiang, Facile synthesis of graphene-supported Ni-CeO_x nanocomposites as highly efficient catalysts for hydrolytic dehydrogenation of ammonia borane, Nano Res., 11 (2018) 4412–4422.
[22] Y.-H. Zhou, S. Wang, Z. Zhang, N. Williams, Y. Cheng, J. Gu, Hollow nickel–cobalt layered double hydroxide supported palladium catalysts with superior hydrogen evolution activity for hydrolysis of ammonia borane, ChemCatChem; European Soc. J. Catal., 10 (2018) 3206–3213.
[23] Y. Jiang, X. Zhang, X. Dai, Q. Sheng, H. Zhuo, J. Yong, Y. Wang, K. Yu, L. Yu, C. Luan, H. Wang, Y. Zhu, X. Duan, P. Che, In situ synthesis of core–shell Pt–Cu frame@metal–organic frameworks as multifunctional catalysts for hydrogenation reaction, Chem. Mater., 29 (2017) 6336–6345.
[24] Y. Guo, T. Park, J.W. Yi, J. Henzie, J. Kim, Z. Wang, B. Jiang, Y. Bando, Y. Sugahara, J. Tang, Y. Yamauchi, Nanoarchitectonics for transition-metal-sulfide-based electrocatalysts for water splitting, Adv. Mater., 31 (2019) 1807134, doi: 10.1002/adma.201807134.
[25] Y. Guo, J. Tang, H. Qian, Z. Wang, Y. Yamauchi, One-pot synthesis of zeolitic imidazolate framework 67-derived hollow Co_3S_4@MoS_2 heterostructures as efficient bifunctional catalysts, Chem. Mater., 29 (2017) 5566–5573.
[26] Y. Guo, J. Tang, Z. Wang, Y.-M. Kang, Y. Bando, Y, Yamauchi, Elaborately assembled core-shell structured metal sulfides as a bifunctional catalyst for highly efficient electrochemical overall water splitting, Nano Energy, 47 (2018) 494–502.
[27] H. Duan, Y. Tian, S. Gong, B. Zhang, Z. Lu, Y. Xia, Y. Shi, C. Qiao, Effects of crystallite sizes of Pt/HZSM-5 zeolite catalysts on the hydrodeoxygenation of guaiacol, Nanomaterials, 10 (2020) 2246, doi: 10.3390/nano10112246.
[28] J. Oenema, J. Harmel, R. Pérez Vélez, M.J. Meijerink, W. Eijsvogel, A. Poursaeidesfahani, T.J.H. Vlugt, J. Zečević, K.P. de Jong, Influence of nanoscale intimacy and zeolite micropore size on the performance of bifunctional catalysts for *n*-heptane hydroisomerization, ACS Catal., 10 (2020) 14245–14257.
[29] A.S.B.M. Najib, M. Iqbal, M.B. Zakaria, S. Shoji, Y. Cho, X. Peng, S. Ueda, A. Hashimoto, T. Fujita, M. Miyauchi, Y. Yamauchi, H. Abe, Active faceted nanoporous ruthenium for electrocatalytic hydrogen evolution, J. Mater. Chem. A, 8 (2020) 19788–19792.
[30] Z.-L. Wang, K. Sun, J. Henzie, X. Hao, C. Li, T. Takei, Y.-M. Kang, Y. Yamauchi, Spatially confined assembly of monodisperse ruthenium nanoclusters in a hierarchically ordered carbon electrode for efficient hydrogen evolution, Angew. Chem. Int. Ed. Engl., 57 (2018) 5848–5852.
[31] Z. Zhang, K. Yao, L. Cong, Z. Yu, L. Qu, W. Huang, Facile synthesis of a Ru-dispersed N-doped carbon framework catalyst for electrochemical nitrogen reduction, Catal. Sci. Technol., 10 (2020) 1336–1342.
[32] B. Zheng, L. Ma, B. Li, D. Chen, X. Li, J. He, J. Xie, M. Robert, T.-C. Lau, pH universal Ru@N-doped carbon catalyst for efficient and fast hydrogen evolution, Catal. Sci. Technol., 10 (2020) 4405–4411.
[33] X. Yang, X. Wang, J. Qiu, Aerobic oxidation of alcohols over carbon nanotube-supported Ru catalysts assembled at the interfaces of emulsion droplets, Appl. Catal., A, 382 (2010) 131–137.
[34] M.A. Watzky, R.G. Finke, Transition metal nanocluster formation kinetic and mechanistic studies. A new mechanism when hydrogen is the reductant: slow, continuous nucleation and fast autocatalytic surface growth, J. Am. Chem. Soc., 119 (1997) 10382–10400.
[35] Z. Sun, X. Zhang, Z.L. Na, B. Han, G. An, Synthesis of ZrO_2–carbon nanotube composites and their application as chemiluminescent sensor material for ethanol, J. Phys. Chem. B, 110 (2006) 13410–13414.
[36] H.-B. Dai, Y. Liang, L.-P. Ma, P. Wang, New insights into catalytic hydrolysis kinetics of sodium borohydride from Michaelis–Menten model, J. Phys. Chem. C, 112 (2008) 15886–15892.
[37] S.U. Jeong, R.K. Kim, E.A. Cho, H.-J. Kim, S.-W. Nam, I.-H. Oh, S.-A. Hong, S.H. Kim, A study on hydrogen generation from $NaBH_4$ solution using the high-performance Co-B catalyst, J. Power Sources, 144 (2005) 129–134.
[38] Q. Zhang, Y. Wu, X. Sun, J. Ortega, Kinetics of catalytic hydrolysis of stabilized sodium borohydride solutions, Ind. Eng. Chem. Res., 46 (2007) 1120–1124.
[39] H. Song, Y. Cheng, B. Li, Y. Fan, B. Liu, Z. Tang, S. Lu, Carbon dots and RuP_2 nanohybrid as an efficient bifunctional catalyst for electrochemical hydrogen evolution reaction and hydrolysis of ammonia borane, ACS Sustainable Chem. Eng., 8 (2020) 3995–4002.
[40] H. Wang, L. Zhou, M. Han, Z. Tao, F. Cheng, J. Chen, CuCo nanoparticles supported on hierarchically porous carbon as

catalysts for hydrolysis of ammonia borane, J. Power Sources, 651 (2015) 382–388.
[41] H. Liang, G. Chen, S. Desinan, R. Rosei, F. Rosei, D. Ma, In situ facile synthesis of ruthenium nanocluster catalyst supported on carbon black for hydrogen generation from the hydrolysis of ammonia-borane, Int. J. Hydrogen Energy, 37 (2012) 17921–17927.
[42] K. Yang, L. Zhou, G. Yu, X. Xiong, M. Ye, Y. Li, D. Lu, Y. Pan, M. Chen, L. Zhang, D. Gao, Z. Wang, L. Zheng, H. Liu, Q. Xia, Ru nanoparticles supported on MIL-53 (Cr, Al) as efficient catalysts for hydrogen generation from hydrolysis of ammonia borane, Int. J. Hydrogen Energy, 41 (2016) 6300–6309.
[43] N. Cao, W. Luo, G. Cheng, One-step synthesis of graphene supported Ru nanoparticles as efficient catalysts for hydrolytic dehydrogenation of ammonia borane, Int. J. Hydrogen Energy, 38 (2013) 11964–11972.